

OPEN ACCESS

EDITED BY

Khameel B. Mustapha. University of Nottingham Malaysia Campus,

REVIEWED BY

Davood Rahmatabadi, University of Tehran, Iran Ngnassi Djami Aslain Brisco, University of Ngaoundéré, Cameroon

*CORRESPONDENCE

Moises Jimenez-Martinez.

RECEIVED 22 September 2025 REVISED 15 October 2025 ACCEPTED 17 October 2025 PUBLISHED 10 November 2025

Jimenez-Martinez M Varela-Soriano J Carrera-Espinoza R and Coca-Gonzalez M (2025) Post-treatment to enhance the mechanical performance of printed Onyx. Front. Mech. Eng. 11:1710902. doi: 10.3389/fmech.2025.1710902

© 2025 Jimenez-Martinez, Varela-Soriano, Carrera-Espinoza and Coca-Gonzalez. This is an open-access article distributed under the terms of the Creative Commons Attribution License (CC BY). The use, distribution or reproduction in other forums is permitted, provided the original author(s) and the copyright owner(s) are credited and that the original publication in this journal is cited, in accordance with accepted academic practice. No use, distribution or reproduction is permitted which does not comply with these terms.

Post-treatment to enhance the mechanical performance of printed Onyx

Moises Jimenez-Martinez^{1*}, Julio Varela-Soriano¹, Rafael Carrera-Espinoza² and Manuel Coca-Gonzalez¹

¹Tecnologico de Monterrey, Escuela de Ingeniería y Ciencias, Puebla, Mexico, ²UDLAP, Ex-Hacienda Santa Catarina Mártir S/N Ex-Hacienda Santa Catarina Martir Ex-Hacienda Santa Catarina Mártir, Puebla, Mexico

Additive manufacturing has high potential to achieve a low carbon footprint because it offers the possibility of fabricating components without using manufacturing tooling. However, the mechanical properties of printed components need improvement. The flexibility of the designs generated by controlling the input of the material during filament extrusion in additive manufacturing allows the fabrication of components without tools; however, crystallization occurs because of the temperature gradient in the printed layers and the layers added during printing. Temperature governs polymer crystallization kinetics. Because the material extrusion process is nonisothermal at the welding interface, polymer crystallization kinetics and degree of crystallization are determined by the thermal history developed during manufacturing. Crystallization worsens the mechanical properties because internal forces are concentrated due to the residual stresses present during cooling. There is a wide range of literature and research on the effect of post-heat treatment on improving mechanical properties in metals. To the best of our knowledge, studies on the post-processing of 3D-printed polymers are limited. This research proposes post-processing to homogenize the structure of the printed component through thermal treatment to improve the ultimate tensile strength of Onyx. Annealing and normalizing treatments almost doubled the mechanical strength of raw printed Onyx.

KEYWORDS

post-treatment, additive manufacturing, Onyx, annealing, normalizing

1 Introduction

Since its introduction, 3D printing has been used to develop prototypes using additive techniques such as stereolithography, selective laser sintering, digital light process, multi-jet fusion, PolyJet, direct metal laser sintering, electron beam melting, and material extrusion (Wu et al., 2023). Additive manufacturing (AM) with material extrusion is one of the most commonly used printing technologies. AM generates a 3D component layer by layer, and the physical printing configurations and manufacturing parameters are chosen depending on the printing configuration and geometry. In AM, the gradient temperature is changed during the printing and cooling stages after the material is extruded and deposited on the layer; this temperature history affects the mechanical performance of the printed component. This manufacturing technology is versatile, as the printing parameters such as stacking sequence, raster angles, nozzle temperature, and layer height can be customized. The position and alignment of the printed layers and the overall parameters affect the

mechanical strength parameters such as material stiffness (Young's modulus), strain, and ultimate tensile strength (Sangaletti et al., 2024; El Essawi et al., 2024).

Some filament materials used as matrix materials in 3D printing are polylactic acid (PLA), acrylonitrile butadiene styrene (ABS), thermoplastic polyurethane (TPU), glycol-modified polyethylene terephthalate (PETG), and a nylon-reinforced fiber known as Onyx; the component to be printed can be reinforced with fibers such as Kevlar, glass fiber, and carbon fiber (Rahmatabadi et al., 2024; Soltanmohammadi et al., 2024). Onyx allows generating novel structures based on low production volumes, by design, resistance, and failure processes (Lin et al., 2024). Onyx has the potential to develop components that can withstand dynamic loads, having a resistance to mechanical fatigue (Jimenez-Martinez et al., 2023). Similarly, mechanical impact absorbers have been proposed, with the ability to have a percentage of recovery in the process of energy absorption (Jimenez-Martinez et al., 2025).

The implementation of additive manufacturing enables the manufacturing of low production volumes without the need for special tools. However, the same flexibility results in areas of opportunity for qualitative and quantitative aspects. Among them are surface finish, precision, and lower mechanical properties (Sawant et al., 2023). The advantages of 3D printing include ease of manufacturing complex geometries, but the components generally have poor mechanical properties because of the anisotropic behavior generated by printing defects between layers and defects such as air voids and poor bonding. These shortcomings influence the microstructure and mechanical properties of the printed component (Eren et al., 2023; Bayati et al., 2025).

The mechanical strength of a polymer can be improved by post-processing. As part of the post-processing, physical and structural aspects of the component are improved by developing a drying process, improving the adhesion of the printed layers by reducing the porosity (Pascual-González et al., 2024). The mechanical behavior of the printed polymer components is influenced by post-printing treatments that have a physical effect on both the surface finish and the mechanical properties. Some treatments can be chemical or thermal, such as coatings, polishing, sandblasting, and steam smoothing (Khosravani et al., 2023a).

Szust and Adamski increased the tensile strength of printed polyethylene terephthalate (PET) components three times using post-treatments (Szust and Adamski, 2022). Sanding improves the surface roughness between 3% and 25%, having an impact not only on the surface finish but also on the precision (Sawant et al., 2023). Another process to improve the performance is the infiltration, which increases the mechanical resistance up to 10% (Ayres et al., 2019). Acetone and its vapors have been used to modify the surface finishing and the mechanical properties in components of printed acrylonitrile butadiene styrene (ABS) (Khosravani et al., 2023a; Aguilar et al., 2024).

Jimenez-Martinez et al. enhanced the fatigue life of printed PLA (Jimenez-Martinez et al., 2024); this improvement was consistent with the results reported by Ramalingam et al. (2021). In both studies, the mechanical performance of printed components was enhanced through post-heat treatment. Thermal treatment involves heating the component to a specified temperature and then cooling it with different ramps and media. Temperature governs the polymer crystallization kinetics. Because the material extrusion

process is a non-isothermal process at the welding interface, polymer crystallization kinetics and degree of crystallization are determined by the thermal history. Moreover, the impedance of crystallization for semi-crystalline polymer across the welding interface causes poor weld quality, which further deteriorates the mechanical performance (Rabbi et al., 2021; Nikiema et al., 2023a; Vorkapić et al., 2022).

The mechanical properties of printed parts are poorer than those of other additive materials formed by methods such as injection; printed parts have approximately 30% less strength, reducing the feasibility of using these parts as structural components. The mechanical behavior depends on crystallinity and deals with the anisotropy of the component. The problems caused by the effect of the thermal history between different filament layers and voids can be reduced by post-treatment. This process is a numerical function $x \to U_x$ of a variable (X_s) , where the variable may be temperature, cooling ramps, cooling time, cooling medium, or configuration space; for example, the oven chamber space and its characteristics. The optimum range of auxiliary heating temperature is between the glass transition temperature (Tg) and melting temperature, which is lower than the degradation temperature (Yu et al., 2020; Goo et al., 2020). The mechanical performance of the polymers is a function of the manufacturing process that generates a specific lamellar thickness, and crystallinity is represented by the microstructural section of the component. Complete crystallization is allowed to standardize the full volume; the degree of crystallinity (X_c) is the amount of the crystal material in the space (ξ). When crystallization is completed, $X_C = 1$; otherwise, it is expressed by Equation 1 as follows depending on the maximum crystallinity at the time of completion of spacefilling $X_{C\infty}$:

$$X_C = \xi \cdot X_{C\infty} \tag{1}$$

Using a post-treatment, the crystalline state is modified by a secondary crystallization process. Isothermal crystallization depends on time, temperature, and cooling rate (Parodi et al., 2017; Delbart et al., 2023).

The degree of crystallinity can be described by Equation 2 as follows:

$$X_C = \frac{1}{w} \frac{\Delta H_m - \Delta H_c}{\Delta_m^0} \tag{2}$$

where ΔH_m is the enthalpy of fusion; ΔH_c is the enthalpy of cold recrystallization; Δ_m^0 is the enthalpy of fusion for 100% crystalline; w is the mass fraction.

The temperature used in the thermal treatment promotes spherulite nucleation and growth, and the temperature can be set between the glass transition temperature and the extrusion temperature because minimal thermal degradation occurs at the printing temperature (Das et al., 2021). Cooling time is the key factor in post-heat treatment. The temperature range is defined by the temperature reached during the thermal treatment and the time for which it is maintained; under this assumption, different strengths or ductilities can be achieved by manipulating the time duration by considering the crystallinity along with the cooling process (Chapman et al., 2021). Thermal history generates and controls the structure crystallinity (Riggins et al., 2024). To bridge this gap,

researchers have explored thermal post-treatments, such as annealing and normalizing, to relieve internal stresses, promote polymer crystallization, and improve interlayer adhesion in printed Onyx and analogous polyamide 6 (PA6) carbon fiber composites. The expected 3D printed properties are poorer than those achieved by traditional methods because of the inhomogeneous building in 3D printing, generating a brittle structure.

Annealing involves heating the printed part to an elevated temperature, typically between the polymer's glass transition and melting point, for a period, then cooling slowly. For semi-crystalline polymers like nylon (PA6), this can increase crystalline phase content and allow polymer chains at layer interfaces to diffuse and re-bond, strengthening the part. In the case of PA6-based composites, optimal annealing is often done near the PA6 melting point. Handwerker et al. (2021) report that annealing PA6 composites for ~ 6 h at ≈ 200 °C (around PA6's melt temperature) yielded the greatest improvements in mechanical performance. In the study, annealing led to a three-fold increase in Young's modulus and a 50% increase in ultimate tensile strength (UTS). A critical mechanism behind these improvements is increased polymer crystallinity and improved fiber-matrix interaction after heat treatment. The strength/stiffness gains are attributed to better interlayer fusion and reduced defects: at 200 °C anneal, many internal voids were eliminated, though some porosity remained and contributed to embrittlement (Equation 3, 4). This embrittlement phenomenon is commonly reported: as parts become more crystalline and less ductile, tensile elongation at break tends to drop (Kechagias et al., 2025).

Tujmer and Pilipović (2025) observed more moderate but still significant gains in short carbon fiber PA6 prints: with proper annealing, tensile strength improved by up to 16.7%, and tensile modulus improved by up to 35%. Their statistical analysis confirmed temperature as the dominant factor. Higher annealing temperatures (110 °C–170 °C) produced better strength/stiffness outcomes than lower temperatures or shorter times. In fact, the highest gains in their work occurred at 170 °C (near PA6's softening point \sim 180 °C), although they caution this is close to the point where the nylon matrix begins to soften and risks dimensional deformation. Thus, annealed Onyx/PA6-CF prints are stiffer and often stronger but also more brittle than as-printed parts.

A post-heat treatment is proposed to improve the mechanical properties. Two types of thermal treatments were performed: annealing and normalizing. Normalizing at 135 $^{\circ}$ C makes it possible to increase the tensile strength to almost 90% of the ultimate tensile strength (*UTS*), whereas annealing at the same temperature increased *UTS* to 110%.

Thus, the novelty of this study lies in directly analyzing the behavior of Onyx in its pure form, without reinforcement, because, to the best of the author's knowledge, most current studies only analyze metals or similar materials and not printed polymers.

2 Materials and methods

A Markforged Mark Two printer was used to fabricate all the specimens in this study. The filament used was Onyx (diameter: 1.75 mm; color: black). Onyx has a nylon matrix reinforced with random short carbon fibers (Li et al., 2024). Although the type of

nylon used in Onyx is not specified by the brand, Huang et al. suggested that it is Polyamide 6, which has a melting point of 221.7 °C (Khan and Ahmed, 2015). However, it is mixed with a carbon fiber of diameter 7 μm, and its printing temperature is 273 °C. Figure 1 shows the schematic printer with two nozzles: one for the matrix and one for the fiber reinforcement. In this study, only the matrix nozzle is used because the main target is to analyze the thermal treatment effect on the mechanical performance of Onyx, as the final printed component, without reinforcement. The matrix material has an isolation chamber to prevent humidity absorption. This polymer reacts with oxygen during melting and extrusion in the nozzle, causing undesirable oxidation and degradation of the material. Onyx is made mainly of nylon, which absorbs more water than other materials such as PLA. The humidity absorption of filaments influences the saturation level, which is highly dependent on humidity and temperature, and hence, it affects the crystallinity process and worsens the mechanical performance by plasticization (Nikiema et al., 2023a).

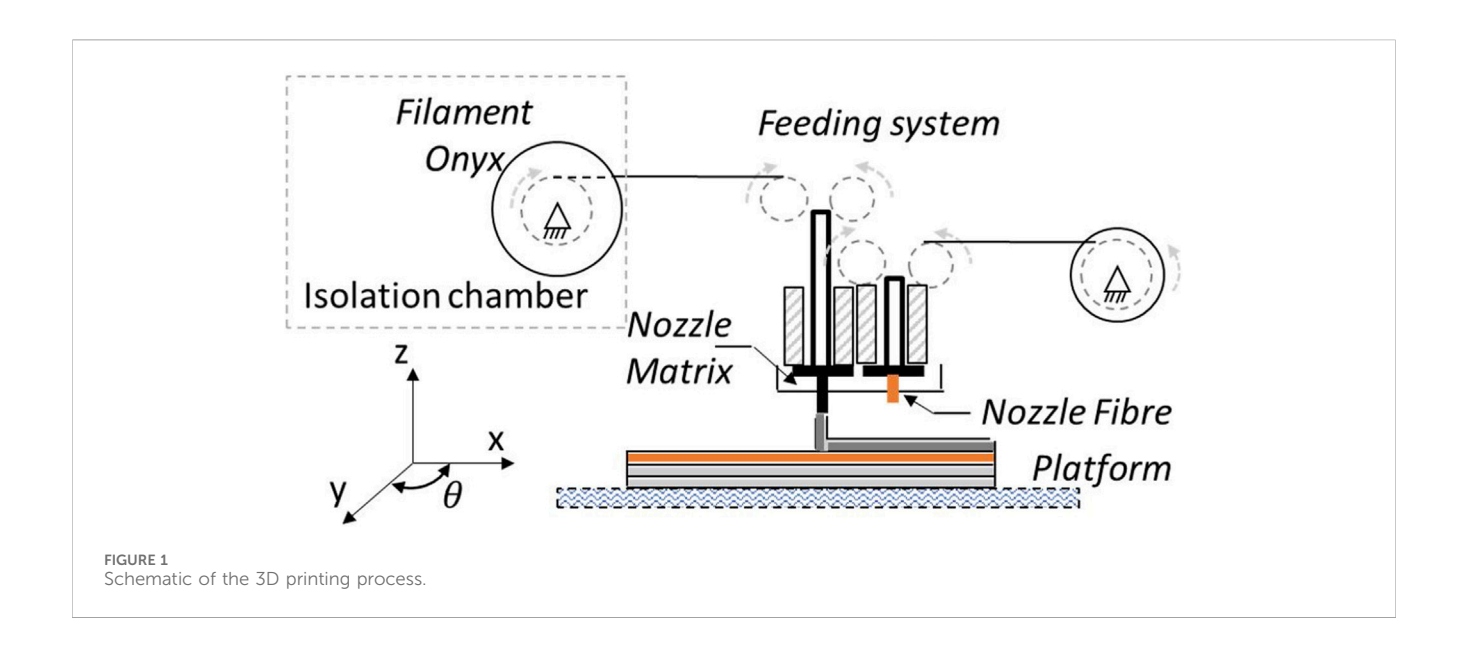
The test component has a dog bone geometry based on ASTM D638 type 1. The gauge is 3.2 mm thick, and the calibrated length, width and total length are 50 mm, 13 mm, and 165 mm, respectively, as shown in Figure 2.

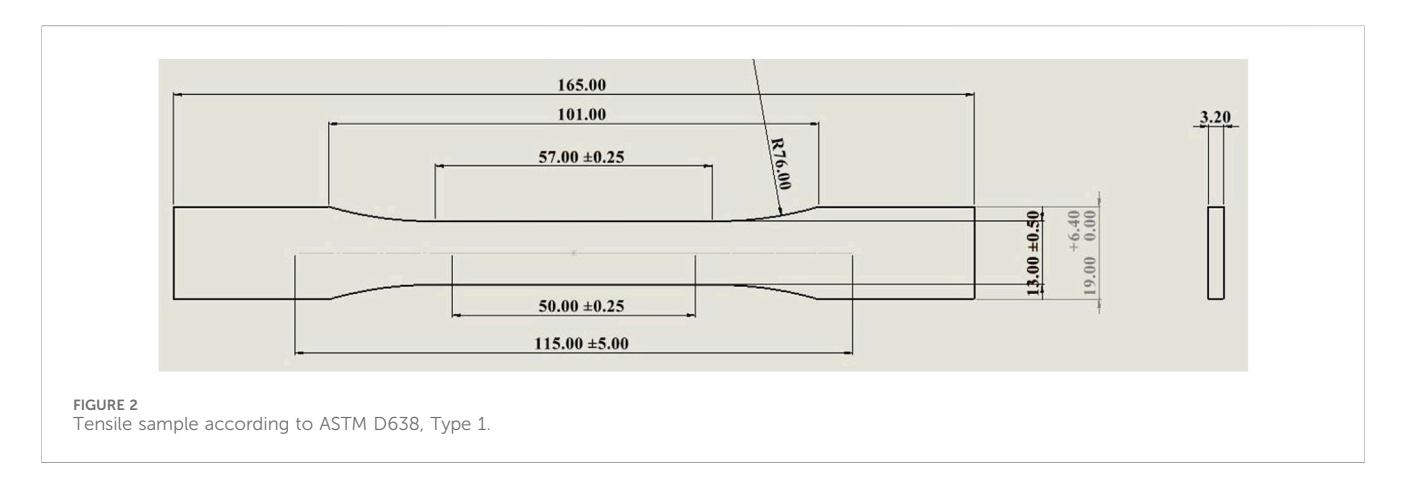
The model was developed using Catia software and exported to Stl files (STereoLithography). The customized printing parameters were as follows: an infill percentage of 100%, no reinforcement, a layer height of 0.1 mm, a printing process involving 32 layers, raster of 45°, no support with two wall layers, and an extrusion temperature of 273 $^{\circ}$ C (Nikiema et al., 2024; Coca-Gonzalez et al., 2025).

Once printed, the components were allowed to cool to room temperature and kept in a confined space before beginning the thermal process. Humidity is not considered, even though Onyx, which is made of nylon, is sensitive to moisture absorption. However, this effect occurs after 165 days of exposure, absorbing 2% and reducing the stiffness of the component by 50%–65% (Nikiema et al., 2023a; Faust et al., 2021). Annealing and normalizing were performed using a Thermolyne furnace model FA1740-1 (Figure 3) with a programmable temperature controller to ensure calibration and instrumented with thermocouples. Once the desired temperature was reached, the oven was left empty for 2 h to ensure uniform temperature.

The chamber was preheated to the desired temperature. The thermal annealing and normalization protocols are shown in Figure 4. In the case of normalization, at the end of the treatment time, the part is removed from the furnace, allowing the cooling process to be carried out based on the temperature of the room. In the annealing case, upon the conclusion of the treatment, the furnace is turned off, leaving the component to be cooled inside. This protocol is considered the normal cooling procedure. The mechanical tests were performed at the end of the cooling process. They were applied to all samples unless explicitly stated otherwise.

The Markforged printer has several printing variables that are set using its Eiger software. Some printing parameters that can be customized are layer thickness, number of walls, raster angle, deposition (concentric, isotropic), and type of infill patterns (triangular, rectangular, hexagonal, gyroid, or solid). Nikiema et al. reported in 2023 (Nikiema et al., 2023b) and in 2024 (Nikiema et al., 2024) the effect of the number of walls on the Young's modulus of Onyx printed materials. The objective of the





present study is to compare the effect of heat treatment in the two-wall configuration. All the specimens were printed with a 100% solid pattern density, with successive perpendicular layers (Figure 5). Figure 5A shows the odd layers, and the next layer is longitudinal for the even layers (Figure 5B).

A uniaxial tensile test was conducted in this study. This test was conducted using an Instron universal machine, which has a Blue Hill controller in which measurements are made at a sampling frequency of 0.2 s (Figure 6). Although the test speed was determined based on several tests according to ASTM D638 and a rate of displacement of 1.25 mm/min, different velocities were evaluated to analyze the effects achieved by varying rates from 10 mm/min to 70 mm/min (Nikiema et al., 2024; Fisher et al., 2023).

The following Equations 3 and 4 show the calculations done for the graphs obtained from the signals as force and displacement.

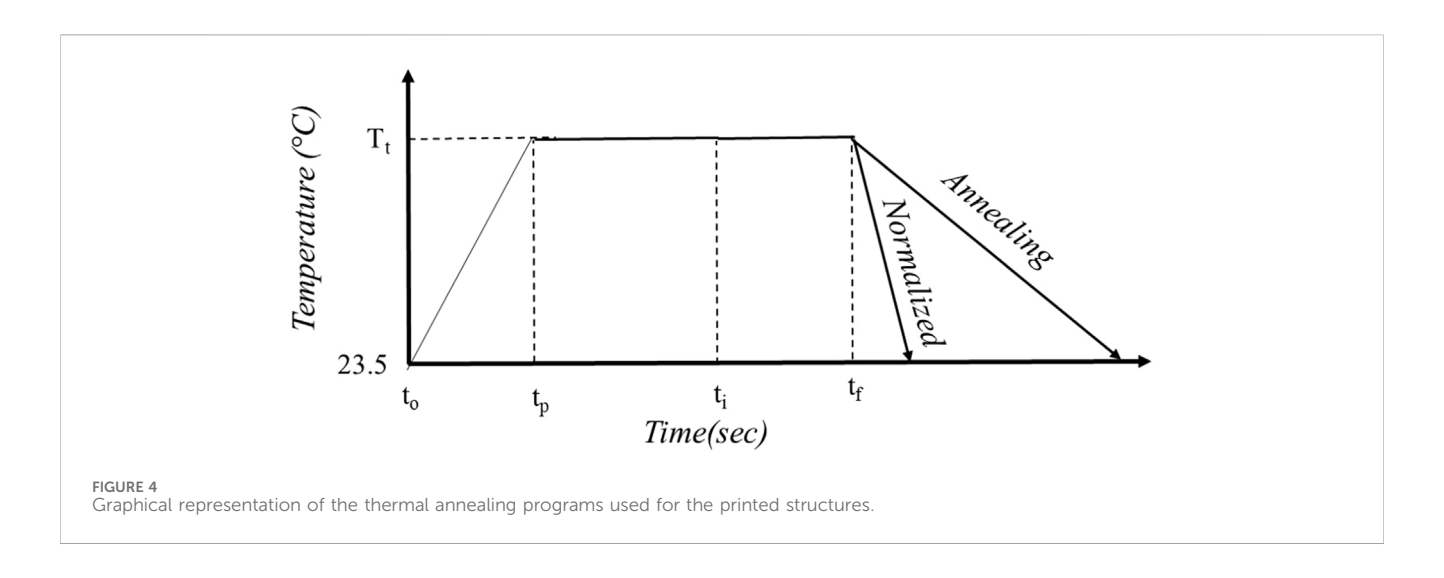
$$\sigma_s = F/A_o \tag{3}$$

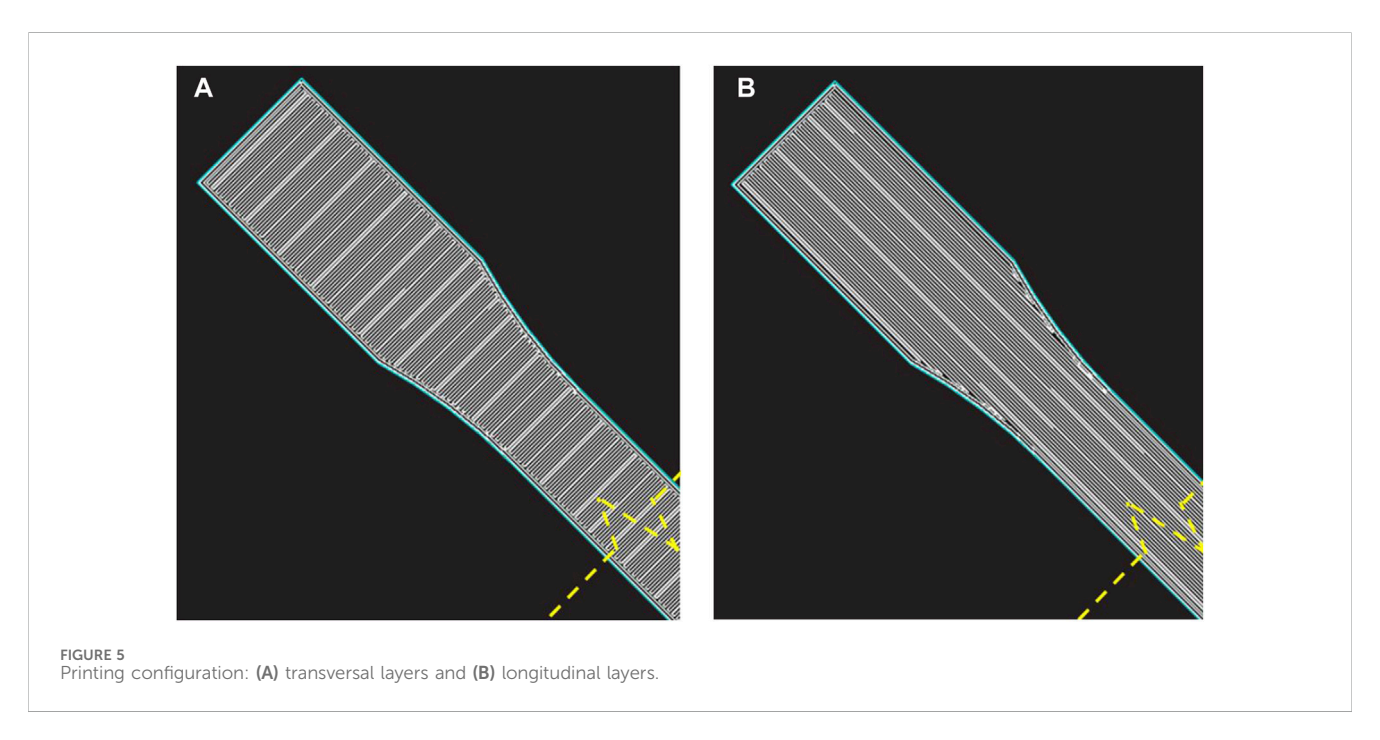
$$\varepsilon = \delta L/L \tag{4}$$

where F is the force applied during each test point; A_o is the initial cross-sectional area; L is the gauge length.



FIGURE 3
Heat treatment equipment.





3 Results and discussion

To analyze the effect of the thermal treatment on the printed Onyx, the mean of the UTS in the tensile test was plotted (Figure 7; Table 1).

The results obtained from the raw printed components were UTS = 32.122 MPa and a strain of 0.398. These parameters will be used to evaluate the effect of heat treatments on printed components.

Two time instants were initially used to define the duration for which the components were in the furnace. The time depends on the thickness of the metals. This rule defines that for every inch of thickness there should be 1 h of treatment (Cain, 2003); hence, the time was set as 7 min. A previous study by Jimenez-Martinez et al. (2024) found that one of the best times for a thermal treatment for PLA is the printing time. Due to this, 1.5 h will be evaluated. There are treatment times where the first minute is for the surface, and

then there should be an effect on the core. Therefore, different times will be evaluated.

Due to the variability of the parameters in the printing process, the printing time of the largest cross section is considered important because no supports are used and because of the way the piece is placed on the printing bed. The second time is defined as the printing time. The temperature was set at 50 °C, and the difference was the time in the oven. In addition, annealing and normalization were performed. In the case of 7 min in the oven, there was no difference between the annealed and normalized materials (Figure 8A). For 7 min in the oven, similar results are observed in both treatments. However, setting the component in the oven for 1.5 h caused an increase in the mechanical resistance during annealing compared to normalization. UTS was increased by 28.3% with the annealing treatment, while UTS was marginally improved by 2.368% with a normalized treatment (Figure 8B).



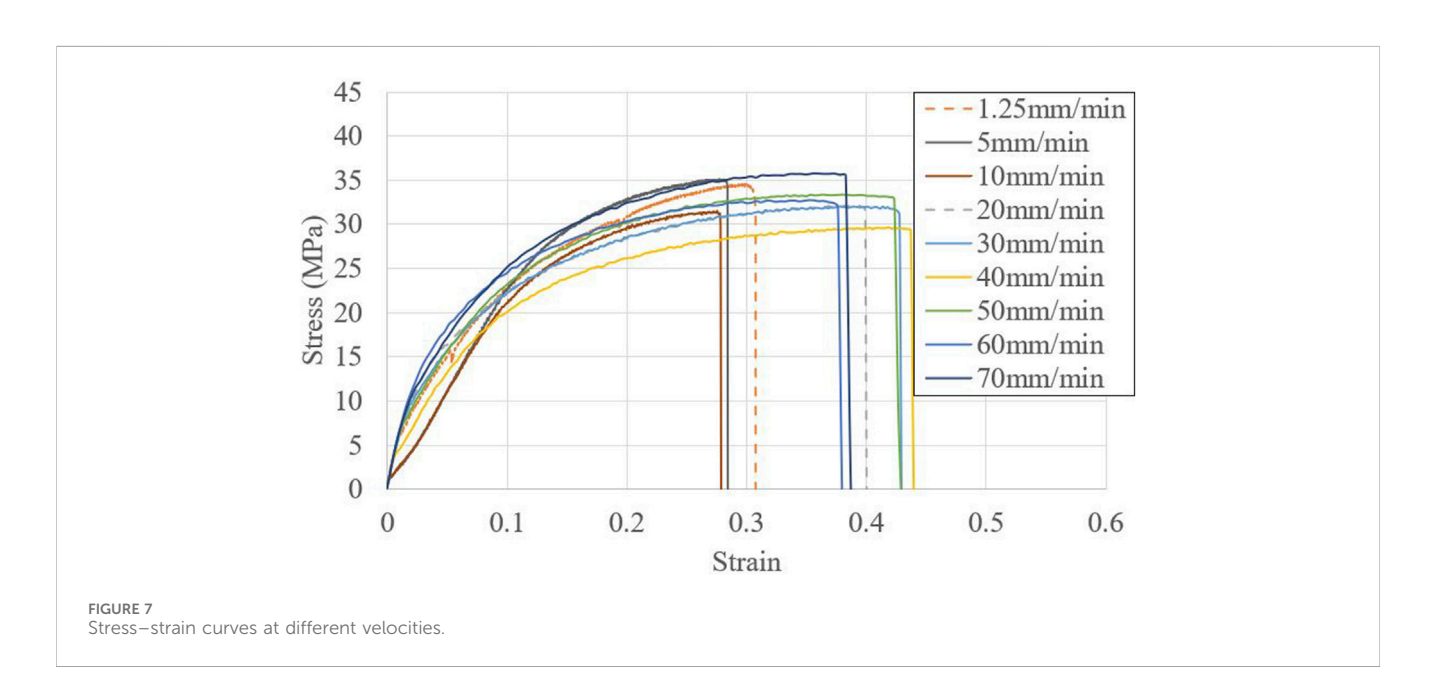
Based on these results, 1.5 h was defined as the ideal period to perform the treatments. To know the temperature ratio, tests were conducted at 60 °C (Figure 9a), and the obtained tendency was similar to that at 50 °C: that is, with annealing, a higher mechanical strength was achieved. The normalized value was only 3% higher than the reference value, while the value after annealing was 43.8% higher than the untreated component. The difference is approximately 10 MPa. By increasing the temperature to 100 °C,

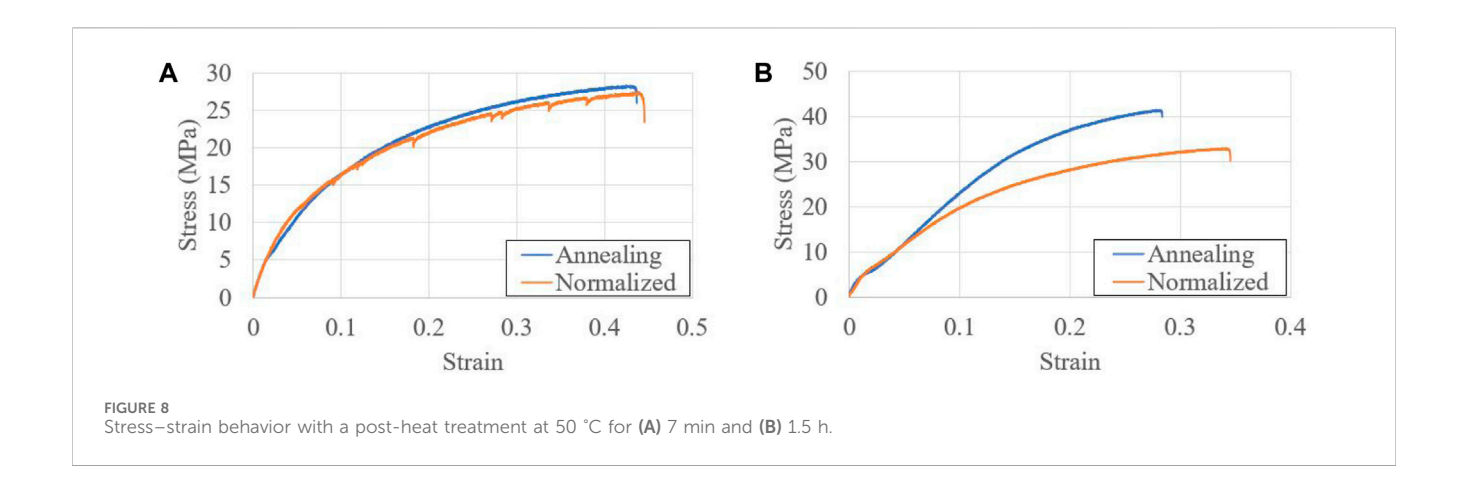
TABLE 1 Tensile test results at different velocities.

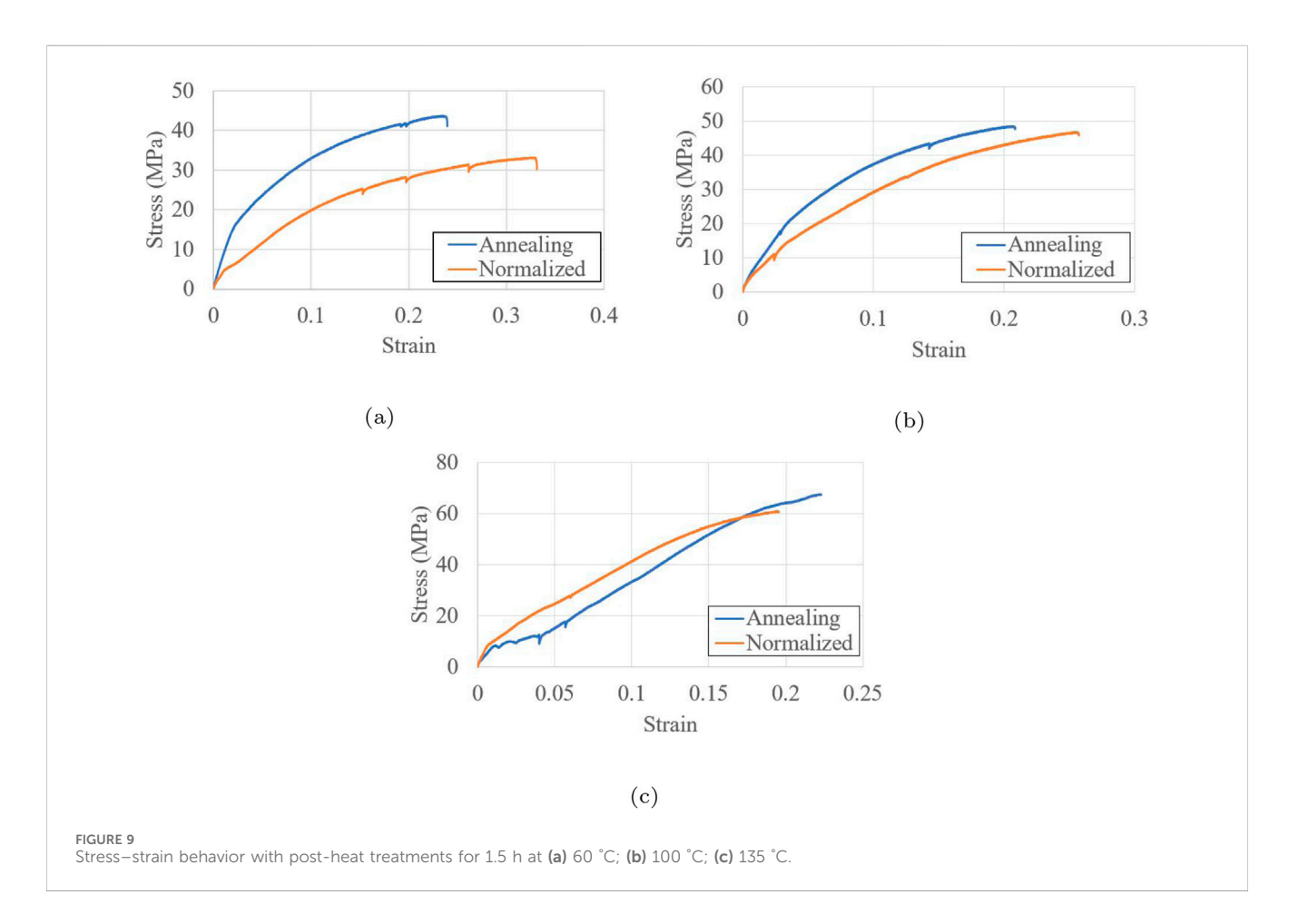
Rate (mm/sec)	UTS (MPa)	Strain at failure		
1.25	34.575	0.30842		
10	26.678	0.239		
20	32.089	0.4113		
30	32.060	0.44566		
40	29.639	0.4825		
50	33.325	0.45526		
60	32.784	4 0.4142		
70	35.825	0.4288		
Mean	32.122 0.3981425			

an improvement of 45% was observed with a standardizing treatment and 51% with annealing (Figure 9b). While applying a temperature of 135 $^{\circ}$ C, an improvement of 89% was achieved after normalizing and 110% after annealing, resulting in more than doubling of the UTS from 32.12 MPa to 67.65 MPa (Figure 9c).

The resulting behavior of the treatment changes depending on the obtained product, while the materials subjected to annealing exhibit increased stiffness and UTS. The materials become brittle, and the deformation at the fault decreases. While normalizing increases the resistance, the product is more ductile than that obtained with annealing but less ductile than the untreated component. This is because recrystallization occurs when a material is cooled slowly or when the material has time to crystallize. During normalization, the rate of cooling is very high, resulting in brittle materials. In contrast, annealing involves a very low rate of cooling or temperature loss, allowing for the greater rearrangement of the crystals and facilitating more plastic deformations depending on the time and temperature of the treatment.





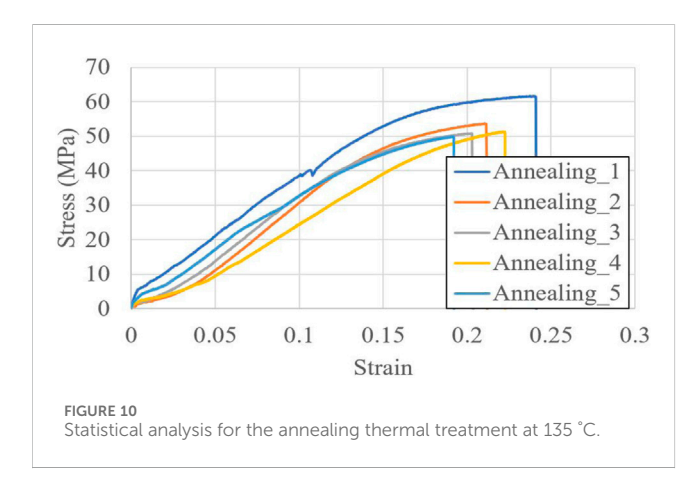


The mechanical strength of polymers can be improved through heat treatments, and the results obtained by normalizing and annealing are consistent with the improvement described by Landel and Nielsen (1993) by applying tensile loads (Wang et al., 2024). Table 2 summarizes the thermal treatments from 50 °C to 135 °C. In the normalized treatment at 50 °C, the increase in resistance is marginal compared with the improvement of 28.5% achieved with annealing. The percentage decrease in deformation is similar to the improvement in resistance when the decrease is approximately half of that achieved with annealing; there is no linear increase in resistance with a decrease in deformation. At 60 °C,

the resistance and annealing deformation improved consistently and decreased, but in normalization, an improvement of only 1% compared to the temperature of 50 $^{\circ}$ C was achieved, but the deformation increased by more than 3%. At 100 $^{\circ}$ C, the strength achieved with a normalizing treatment is ~90% of the strength achieved with annealing. Unlike the previous temperatures, the difference between annealing and normalization treatments is 25%-annealing reduces the deformation, as expected. Of the temperatures evaluated, 135 $^{\circ}$ C corresponded to the best strength achieved with annealing, but the percentage of decrease in deformation was lower than with normalization.

TABLE 2 Ultimate tensile strength as a function of heat treatment.

Temperature ° C	Treatment	UTS (MPa)	% Change	Strain	% Change
23.5	NA	32.122	NA	0.398	NA
50	Annealing	41.298	28.568	0.284	-28.789
50	Normalized	32.882	2.368	0.346	-13.212
60	Annealing	43.853	36.523	0.240	-39.780
60	Normalized	33.154	3.213	0.331	-16.864
100	Annealing	48.546	51.130	0.208	-47.727
100	Normalized	46.767	45.593	0.257	-35.350
135	Annealing	67.651	110.610	0.223	-43.985
135	Normalized	60.760	89.154	0.195	-50.957



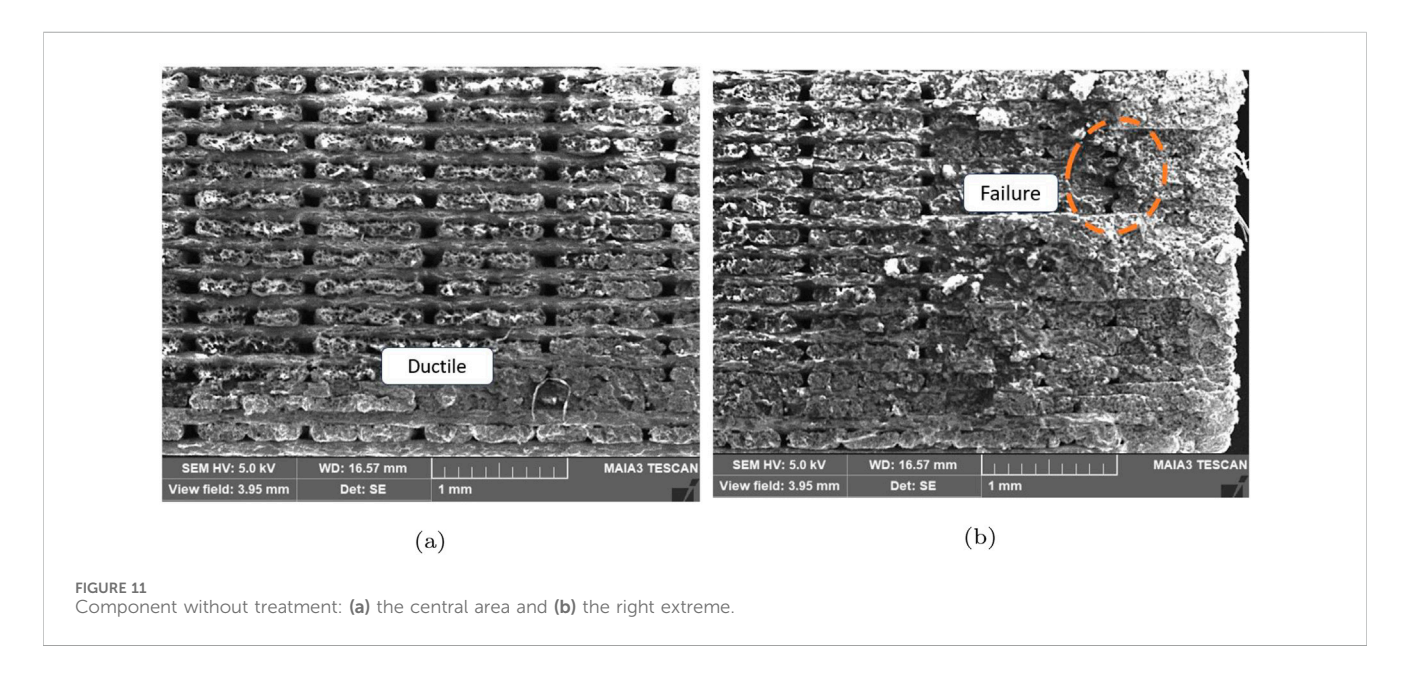
To analyze the reliability of the results, a statistical analysis was performed with five additional tests, as shown in Figure 10. Considering the result of Figure 9c, the mean value of the UTS is

55.88 MPa. Ultimate tensile strength scatter was evaluated using the standard deviation given by Equation 5 as (Ibe and Ibe, 2014)

$$s = \sqrt{\frac{1}{N-1} \sum_{i=1}^{N} (x_i - \mu)^2}$$
 (5)

where μ is the mean value of the UTS, x_i is the sample, and N is the sample number.

The logarithmic standard deviation s=7.148. This is a significant result based on low scatter value (Itu et al., 2019; Vedrtnam et al., 2023; Batley et al., 2024). Comparing the maximum UTS achieved from the annealing treatment of 67.65 MPa with the UTS of non-tensile components of 32.122 MPa, the UTS increased 2.02 times. This UTS value without treatment is similar to that reported by Fisher et al. (2023). Compared to the tensile strength reported by Lee et al., the UTS value of 30 MPa was increased 2.25 times (Lee et al., 2023).



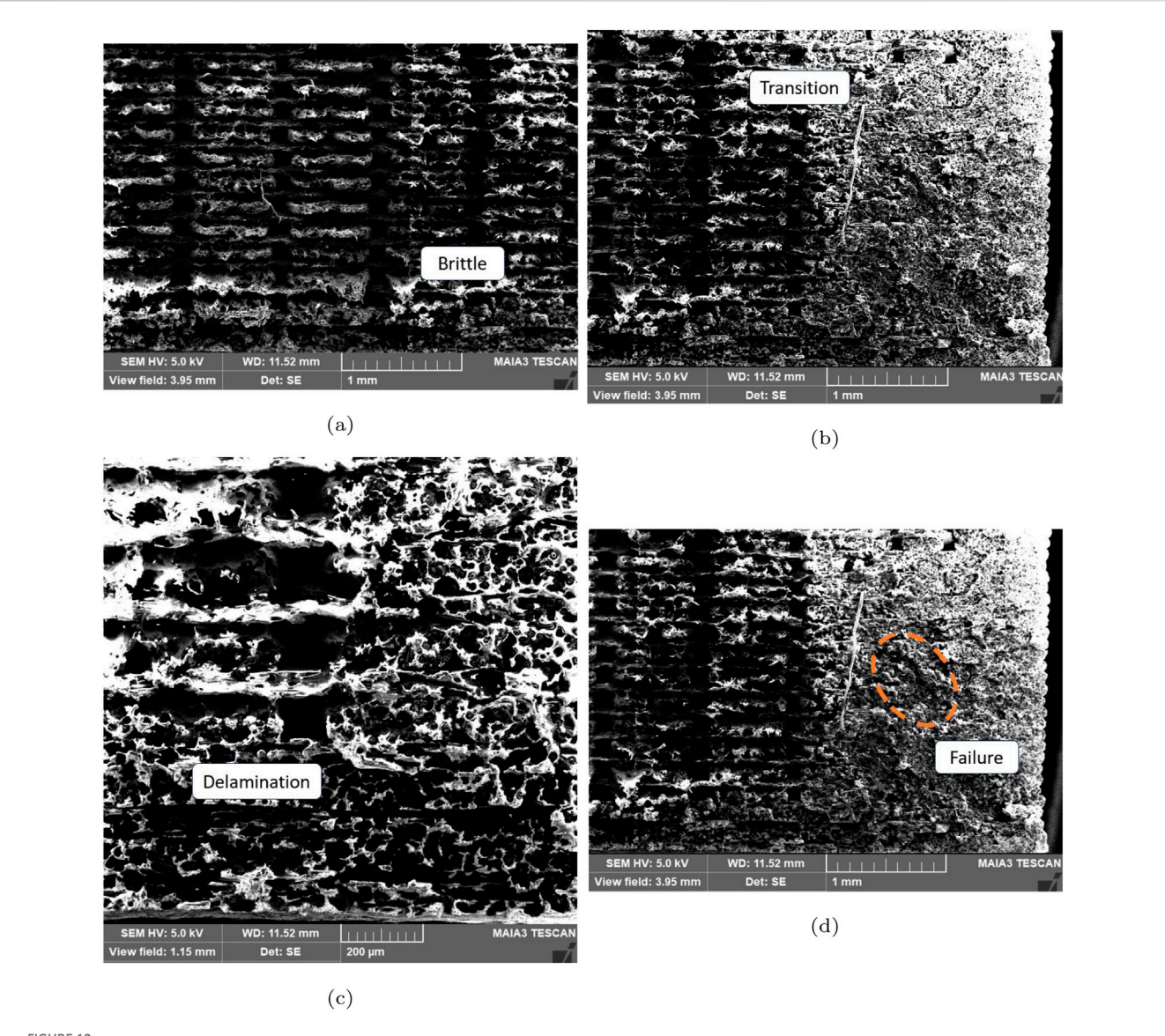


FIGURE 12 Component failure analysis under a normalizing treatment at 50 °C for 7 min: (a) the central part; (b) the right extreme; (c) the transition area between brittle and ductile areas; (d) failure nucleation.

3.1 Scanning electron microscopy

Scanning electron microscopy (SEM) imaging was performed to understand the effect of heat treatment on polymers. In this study, we examined a strong bond with two types of breakage, namely, brittle and ductile (Handbook, 1993).

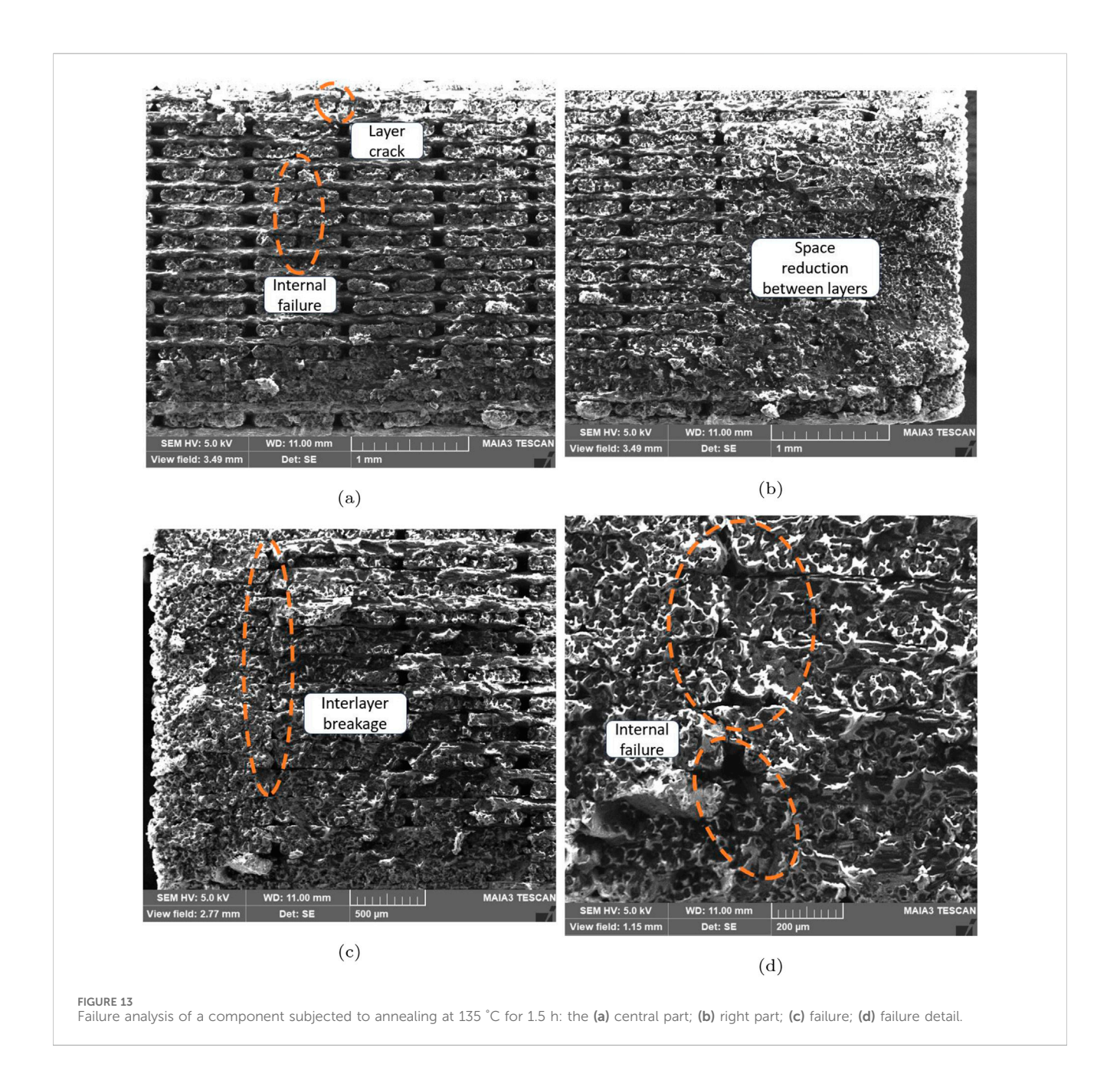
To understand the failure process depending on the time and type of treatment, components were analyzed without heat treatment and with treatment for 7 min at 135 °C, and analyzed with normalizing and annealing.

Figure 11a shows the central area of the component, and Figure 11b shows the end where failure originates and propagates. In the central area, there is a space between longitudinal layers; although these spaces are also observed at the extremes, the main difference is that the upper and lower layers have a fragile fault, while a ductile fault is observed in the center.

Figure 11b shows that these spaces are reduced at the extremes because of the perimeters of the contour. However, the crack is seen in the transition zone between the perimeters and the central zone of the component.

As a result of the treatment, a darker color is observed, as shown in Figure 12a. In addition, Figure 12b shows that the area of the perimeters has a smoother transition between the layers, generating a zone of change from ductile to brittle (Figure 12c). The crack runs in this zone, as seen in Figure 12b and in Figure 14d.

Figure 13 shows the fracture of the specimen subjected to heat treatment at 135 $^{\circ}$ C and annealing for 1.5 H with 59× magnification. Figure 13a shows that the area or areas of greatest fragility at the ends are also reduced, indicating a greater force magnitude than that observed in the previous treatment. Therefore, we speculate that 135 $^{\circ}$ C is the best temperature for this material if the cooling mechanism is modified. Figure 13b shows that the spaces



between the longitudinal layers are reduced because of the combined treatment effect of time and temperature. Failure in this component occurs by separation between the layers (Figure 13c); Figure 13d shows intralaminar and interlaminar failure.

Finally, the component subjected to normalization was treated at 135 °C for 1.5 h. Similar to the case of annealing, the space between longitudinal layers decreased (Figure 14a), improving the mechanical properties because of the availability of a more uniform cross-sectional area. Owing to the resistance of the material, the failure is brittle (Figure 14b), and the failure changes direction, as seen in Figure 14c. Nucleation is observed in Figure 14d.

In accordance with the present results, previous studies have demonstrated that thermal treatment tends to reduce the number of voids, improving the joining process between layers, as shown in Figures 13, 14. These results corroborate the findings of a great deal of the previous work by Huang et al. (2024) and Khosravani et al. (2023b). The mechanism of failure is interlaminar propagation. Although annealing improves the strength, catastrophic failure may occur, changing crack propagation and promoting a brittle failure.

Although nylon's glass transition temperature is 22 °C, Onyx has carbon fiber content, which increases the glass transition temperature of the matrix to 27 °C and has a crystallization temperature of 161 °C (Pascual-González et al., 2020). Gordon reported anomalous behavior for the glass transition, which normally occurs in the first heating cycle. However, when performing a subsequent cycle, it is not observed. If the component is left at rest and a heating cycle is performed again, however, the transition is not only in the same range but has also

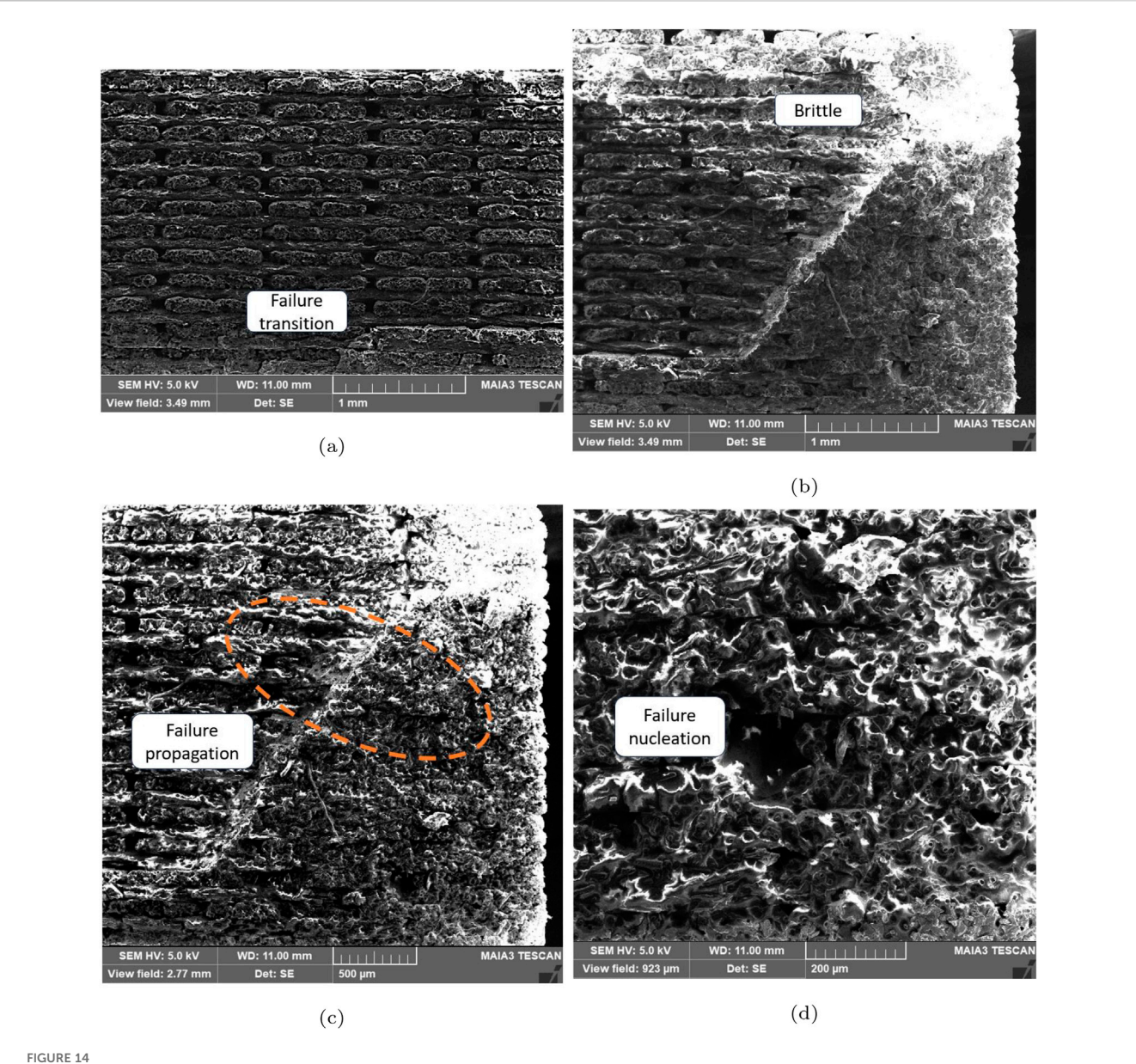


Figure 14 Failure analysis of the component subjected to a normalized treatment at 135 °C for 1.5 h: (a) central part; (b) right part; (c) failure change orientation; (d) failure nucleation.

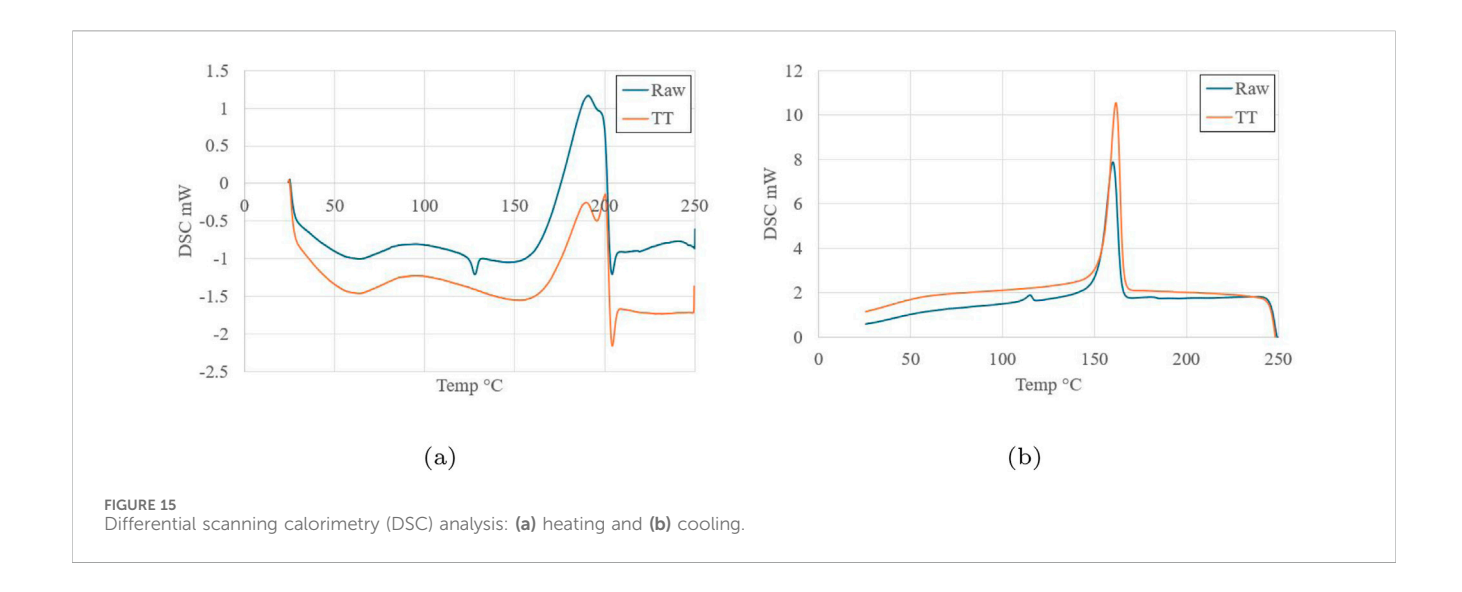
been increased. This is due to the formation of networks by hydrogen bonds, because new cycles of reheating generate new transitions (Gordon, 1971; Klata et al., 2003).

Finally, to understand the effect of the treatment on Onyx printed components, differential scanning calorimetry (DSC) tests were performed with the following characteristics: Atmosphere in air, gas flow 10 mL/min, heating rate 10 °C/min, cooling rate 20 °C/min, raw printed sample 5 mg, and thermally treated sample 6 mg. This comparison of both ramp up and ramp down allows for analyzing the effect of the heat treatment by correlating it with the crystallization process. For the printed part without treatment, a transition is observed at 127 °C and Tm at 202.3 °C (Figure 15a), while in Figure 15b, a transition temperature at 115.9 °C is observed. The crystallization temperature is 158 °C for a raw sample, while it is

162 °C for the treated component. This tendency is eliminated by applying the annealing process in the raw sample, which allows obtaining a more homogeneous structure. Based on the degree of crystallinity shown by the area under the endotherm peak Figure 15b, the crystallinity after annealing treatment has been increased. It improves mechanical strength, as reported on the tensile tests.

The temperature for the treatment should be less than the temperature for the purpose of obtaining dimensional stability. For Onyx, a temperature of 135 °C is suggested. Higher values generate warpage (Coca-Gonzalez and Jimenez-Martinez, 2024). This finding was also reported by Pascual-González et al. (2024).

Based on the transition temperatures observed in the DSC when comparing the cross-sections of the treated components, at a lower



treatment temperature (Figure 12), the spaces between layers cannot be closed, as in the case of treatments at higher temperatures. When comparing the annealing (Figure 13) and normalizing treatment (Figure 14), it is observed that in the former, the cohesion between layers is improved, as was reported by Jimenez-Martinez et al. (2024).

4 Conclusion

This study was conducted to gain deeper insights into the mechanical performance improvement of printed polymer by implementing a post-print process. Heat treatment modifies the morphology of the printed component via recrystallization. This modification allows us to reduce defects and increase the mechanical strength. Through the annealing heat treatment, the ultimate tensile stress of printed Onyx increased more than two times the original value, from 32.12 MPa to 67.61 MPa. The temperature set is 50% of the extrusion temperature, and the time is based on the printing time. Heat treatments above 135 °C are not recommended as this will change the surface finish. The component generates warpage, having a detrimental effect on the mechanical properties.

The manufacture of products from polymers has generally been done through high-volume processes such as compression molding or injection. The use of these materials through additive manufacturing opens an area of opportunity to analyze and implement thermal post-processes typically used in metal fabrication to improve the mechanical properties of the printed items; however, based on the results, an area of opportunity is seen for the generation of applied research in heat treatments in components printed with polymer filaments.

Thermal treatment time is important for this additive manufacturing process, as a temperature gradient persists from the printing of the first layer until the last layer. Because of this, it is important to define the processing time based on the printing time of the largest cross section of the printed component.

Normalization and annealing treatments are adopted. For a given temperature and time spent in the furnace, cooling time

plays an important role in determining the recrystallization process. Short treatment times yield ductile materials, thereby increasing the deformation and reducing component strength. The results show that annealing generally improves the UTS of printed components.

Considerably more work must be done to determine the postthermal treatment effect of Onyx when it is reinforced with carbon fiber, glass fiber, or Kevlar. It is necessary to evaluate the effect of the treatment not only on the core of the material or reinforcement but also on the transition zone and evaluate the cohesion effects, ensuring a robust improvement.

It is emphasized that further research is required to add to the limited literature review on the post-thermal treatment in printed polymers, extend and validate the findings of this study, and assess other material properties, such as toughness, where these types of parameters might affect the suitability of printed Onyx for different engineering applications.

To strengthen the statistical reliability, further studies should investigate the mechanical strength under cyclic loads. In dynamic load cases such as mechanical fatigue, the effects of heat treatment on failure propagation processes could be evaluated to mitigate brittle failure.

Data availability statement

The original contributions presented in the study are included in the article/Supplementary Material, further inquiries can be directed to the corresponding author.

Author contributions

MJ-M: Conceptualization, Data curation, Formal Analysis, Investigation, Methodology, Supervision, Validation, Writing – original draft, Writing – review and editing. JV-S: Data curation, Writing – original draft. RC-E: Investigation, Writing – original draft. MC-G: Conceptualization, Data curation, Formal Analysis, Writing – review and editing.

Funding

The author(s) declare that financial support was received for the research and/or publication of this article. The authors did not receive support from any organization for the submitted work.

Conflict of interest

The authors declare that the research was conducted in the absence of any commercial or financial relationships that could be construed as a potential conflict of interest.

Generative AI statement

The author(s) declare that no Generative AI was used in the creation of this manuscript.

Any alternative text (alt text) provided alongside figures in this article has been generated by Frontiers with the support of artificial

intelligence and reasonable efforts have been made to ensure accuracy, including review by the authors wherever possible. If you identify any issues, please contact us.

Publisher's note

All claims expressed in this article are solely those of the authors and do not necessarily represent those of their affiliated organizations, or those of the publisher, the editors and the reviewers. Any product that may be evaluated in this article, or claim that may be made by its manufacturer, is not guaranteed or endorsed by the publisher.

Supplementary material

The Supplementary Material for this article can be found online at: https://www.frontiersin.org/articles/10.3389/fmech.2025.1710902/full#supplementary-material

References

Aguilar, F. B. J., Varela-Soriano, J., Medina-Castro, A., Torres-Cedillo, S. G., Cortes-Perez, J., and Jimenez-Martinez, M. (2024). Post-fabrication treatment process for abs printed parts using acetone vapor. *Prog. Addit. Manuf.* 10, 1561–1574. doi:10.1007/s40964-024-00725-7

Ayres, T. J., Sama, S. R., Joshi, S. B., and Manogharan, G. P. (2019). Influence of resin infiltrants on mechanical and thermal performance in plaster binder jetting additive manufacturing. *Addit. Manuf.* 30, 100885. doi:10.1016/j.addma.2019.100885

Batley, A., Glithro, R., Dyer, B., and Sewell, P. (2024). Evaluation of tensile strength and repeatability of 3d printed carbon fiber materials and processes. 3D Print. Addit. Manuf. 11 (5), 1691–1702. doi:10.1089/3dp.2022.0262

Bayati, A., Ahmadi, M., Rahmatabadi, D., Khodaei, M., Xiang, H., Baniassadi, M., et al. (2025). 3d printed elastomers with superior stretchability and mechanical integrity by parametric optimization of extrusion process using taguchi method. *Mater. Res. Express* 12 (1), 015301. doi:10.1088/2053-1591/ada1a6

Cain, T. (2003). Hardening, tempering and heat treatment: for model engineers. Spec. Interest Model Books.

Chapman, G., Pal, A. K., Misra, M., and Mohanty, A. K. (2021). Studies on 3d printability of novel impact modified nylon 6: experimental investigations and performance evaluation. *Macromol. Mater. Eng.* 306 (2), 2000548. doi:10.1002/mame.202000548

Coca-Gonzalez, M., and Jimenez-Martinez, M. (2024). Warpage: causes, manufacturing processes and future challenges: a review. *Proc. Institution Mech. Eng. Part L J. Mater. Des. Appl.* 239, 14644207241285399. doi:10.1177/14644207241285399

Coca-Gonzalez, M., Torres-Cedillo, S. G., Alfaro-Ponce, M., Cortés Pérez, J., Díaz-Montiel, P., and Jimenez-Martinez, M. (2025). Influence of perimeter layers on tension mechanical properties of 3d printed onyx. *Front. Mech. Eng.* 11, 1528516. doi:10.3389/fmech.2025.1528516

Das, A., Etemadi, M., Davis, B. A., McKnight, S. H., Williams, C. B., Case, S. W., et al. (2021). Rheological investigation of nylon-carbon fiber composites fabricated using material extrusion-based additive manufacturing. *Polym. Compos.* 42 (11), 6010–6024. doi:10.1002/pc.26281

Delbart, R., Papasavvas, A., Robert, C., Hoang, T. Q. T., and Martinez-Hergueta, F. (2023). An experimental and numerical study of the mechanical response of 3d printed pla/cb polymers. *Compos. Struct.* 319, 117156. doi:10.1016/j.compstruct.2023.117156

El Essawi, B., Abdallah, S., Ali, S., Mohammed, A. N. A., Susantyoko, R. A., and Pervaiz, S. (2024). Optimization of infill density, fiber angle, carbon fiber layer position in 3d printed continuous carbon-fiber reinforced nylon composite. *Results Eng.* 21, 101926. doi:10.1016/j.rineng.2024.101926

Eren, Z., Burnett, C. A., Wright, D., and Kazancı, Z. (2023). Compressive characterisation of 3d printed composite materials using continuous fibre fabrication. Int. J. Lightweight Mater. Manuf. 6 (4), 494–507. doi:10.1016/j.ijlmm.2023.05.002

Faust, J. L., Kelly, P. G., Jones, B. D., and Roy-Mayhew, J. D. (2021). Effects of coefficient of thermal expansion and moisture absorption on the dimensional accuracy of carbon-reinforced 3d printed parts. *Polymers* 13 (21), 3637. doi:10.3390/polym13213637

Fisher, T., Almeida, J. H. S., Jr, Falzon, B. G., and Kazancı, Z. (2023). Tension and compression properties of 3d-printed composites: print orientation and strain rate effects. *Polymers* 15 (7), 1708. doi:10.3390/polym15071708

Goo, B., Hong, C.-H., and Park, K. (2020). 4d printing using anisotropic thermal deformation of 3d-printed thermoplastic parts. *Mater. and Des.* 188, 108485. doi:10. 1016/j.matdes.2020.108485

Gordon, G. A. (1971). Glass transition in nylons. *J. Polym. Sci. Part A-2 Polym. Phys.* 9 (9), 1693–1702. doi:10.1002/pol.1971.160090911

Handbook, D. F. (1993). Material science. us dep. Energy.

Handwerker, M., Wellnitz, J., Marzbani, H., and Tetzlaff, U. (2021). Annealing of chopped and continuous fibre reinforced polyamide 6 produced by fused filament fabrication. *Compos. Part B Eng.* 223, 109119. doi:10.1016/j.compositesb.2021.109119

Huang, F., Chang, W., Islam, M. S., Wang, J., Jiang, B., Tan, Z., et al. (2024). Microcracking resistance of 3d printed fibre composites at cryogenic temperatures. *Addit. Manuf.* 89, 104307. doi:10.1016/j.addma.2024.104307

Ibe, O. C. (2014). "Chapter 8 - introduction to descriptive statistics," in *Fundamentals of applied probability and random processes*. Editor O. C. Ibe Second edn (Boston: Academic Press), 253–274.

Itu, C., Scutaru, M. L., Modrea, A., and Mihălcică, M. (2019). Traction characteristics for the components of a composite sandwich used to build high-rigidity circular plates. *Procedia Manuf.* 32, 268–277. doi:10.1016/j.promfg.2019.02.213

Jimenez-Martinez, M., Varela-Soriano, J., De La Trinidad-Rendon, J. S., Torres-Cedillo, S. G., Cortés-Pérez, J., and Coca-Gonzalez, M. (2023). Fatigue analysis of printed composites of onyx and kevlar. *J. Compos. Sci.* 8 (1), 12. doi:10.3390/jcs8010012

Jimenez-Martinez, M., Varela-Soriano, J., Carrera-Espinoza, R., Torres-Cedillo, S. G., and Cortés-Pérez, J. (2024). Enhancement of fatigue life of polylactic acid components through post-printing heat treatment. *Designs* 8 (1), 7. doi:10.3390/designs8010007

Jimenez-Martinez, M., Narvaez, G., and Diaz-Montiel, P. (2025). Low cycle fatigue of thin-wall printed onyx in energy absorption. *Heliyon* 11 (2), e42120. doi:10.1016/j. helivon.2025.e42120

Kechagias, J. D., Fountas, N. A., Papantoniou, I., and Vaxevanidis, N. M. (2025). Interlaminar bonding assessment in vertical-oriented filament material extrusion bending specimens. *Int. J. Adv. Manuf. Technol.* 136 (11), 4977–4989. doi:10.1007/s00170-025-15124-7

Khan, A. N., and Ahmed, B. A. (2015). Comparative study of polyamide 6 reinforced with glass fibre and montmorillonite. *Polym. Bull.* 72, 1207–1216. doi:10.1007/s00289-015-1333-4

Khosravani, M. R., Ayatollahi, M. R., and Reinicke, T. (2023a). Effects of post-processing techniques on the mechanical characterization of additively manufactured parts. *J. Manuf. Process.* 107, 98–114. doi:10.1016/j.jmapro.2023.10.018

Khosravani, M. R., Anders, D., and Reinicke, T. (2023b). Effects of post-processing on the fracture behavior of surface-treated 3d-printed parts. CIRP J. Manuf. Sci. Technol. 46, 148–156. doi:10.1016/j.cirpj.2023.08.006

Klata, E., Van de Velde, K., and Krucińska, I. (2003). Dsc investigations of polyamide 6 in hybrid gf/pa 6 yarns and composites. *Polym. Test.* 22 (8), 929–937. doi:10.1016/s0142-9418(03)00043-6

- Landel, R. F., and Nielsen, L. E. (1993). Mechanical properties of polymers and composites. NY, United States: CRC Press.
- Lee, G.-W., Kim, T.-H., Yun, J.-H., Kim, N.-J., Ahn, K.-H., and Kang, M.-S. (2023). Strength of onyx-based composite 3d printing materials according to fiber reinforcement. *Front. Mater.* 10, 1183816. doi:10.3389/fmats.2023.1183816
- Li, J., Xu, S., Durandet, Y., Gao, W., Huang, X., and Ruan, D. (2024). Strain rate dependence of 3d printed continuous fiber reinforced composites. *Compos. Part B Eng.* 277, 111415. doi:10.1016/j.compositesb.2024.111415
- Lin, S., Peng, C., Deng, F., Yin, D., and Ye, B. (2024). Influence of structural geometry on tensile properties and fracture toughness in 3d printed novel structures. *Eng. Fail. Anal.* 161, 108277. doi:10.1016/j.engfailanal.2024.108277
- Nikiema, D., Balland, P., and Sergent, A. (2023a). Study of the mechanical properties of 3d-printed onyx parts: investigation on printing parameters and effect of humidity. *Chin. J. Mech. Eng. Addit. Manuf. Front.* 2 (2), 100075. doi:10.1016/j.cjmeam.2023.100075
- Nikiema, D., Sène, N. A., Balland, P., and Sergent, A. (2023b). Study of walls' influence on the mechanical properties of 3d printed onyx parts: experimental, analytical and numerical investigations. *Heliyon* 9 (8), e19187. doi:10.1016/j.heliyon.2023.e19187
- Nikiema, D., Balland, P., and Sergent, A. (2024). Influence of anisotropy and walls thickness on the mechanical behavior of 3d printed onyx parts. CIRP J. Manuf. Sci. Technol. 50, 185–197. doi:10.1016/j.cirpj.2024.03.002
- Parodi, E., Govaert, L., and Peters, G. (2017). Glass transition temperature versus structure of polyamide 6: a flash-dsc study. *Thermochim. Acta* 657, 110–122. doi:10. 1016/j.tca.2017.09.021
- Pascual-González, C., Iragi, M., Fernández, A., Fernández-Blázquez, J., Aretxabaleta, L., and Lopes, C. (2020). An approach to analyse the factors behind the micromechanical response of 3d-printed composites. *Compos. Part B Eng.* 186, 107820. doi:10.1016/j.compositesb.2020.107820
- Pascual-González, C., Caraballo, J. G. M., Lizarralde, I., Gómez, D. G., and Fernández-Blázquez, J. P. (2024). Additive manufacturing and microstructure effects on thermal and mechanical properties of ply-hybrid carbon and glass fiber composites. *Compos. Part B Eng.* 279, 111446. doi:10.1016/j.compositesb.2024.111446
- Rabbi, M. F., and Chalivendra, V. (2021). Improvement in interfacial fracture toughness of multi-material additively manufactured composites through thermal annealing. *Forces Mech.* 5, 100051. doi:10.1016/j.finmec.2021.100051
- Rahmatabadi, D., Soleyman, E., Bashi, M. F. M., Aberoumand, M., Soltanmohammadi, K., Ghasemi, I., et al. (2024). 4d printing and annealing of petg composites reinforced with short carbon fibers. *Phys. Scr.* 99 (5), 055957. doi:10.1088/1402-4896/ad3b40
- Ramalingam, P. S., Mayandi, K., Balasubramanian, V., Chandrasekar, K., Stalany, V. M., and Munaf, A. A. (2021). Effect of 3d printing process parameters on the impact

strength of onyx-glass fiber reinforced composites. *Mater. Today Proc.* 45, 6154–6159. doi:10.1016/j.matpr.2020.10.467

- Riggins, A. W., Jian, H. Y., and Dadmun, M. D. (2024). Increasing the isotropy of 3d printed poly (ether ether ketone) using a combination of bimodal polymer blends and post-process thermal annealing. *Addit. Manuf.* 84, 104127. doi:10.1016/j.addma.2024. 104127
- Sangaletti, S., Aranda, M. T., Távara, L., and García, I. G. (2024). Effect of stacking direction and raster angle on the fracture properties of onyx 3d printed components: a mesoscale analysis. *Theor. Appl. Fract. Mech.* 129, 104228. doi:10.1016/j.tafmec.2023. 104228
- Sawant, D., Shinde, B., and Raykar, S. (2023). Post processing techniques used to improve the quality of 3d printed parts using fdm: state of art review and experimental work. *Mater. Today Proc.* doi:10.1016/j.matpr.2023.09.202
- Soltanmohammadi, K., Rahmatabadi, D., Aberoumand, M., Soleyman, E., Ghasemi, I., Baniassadi, M., et al. (2024). Effects of tpu on the mechanical properties, fracture toughness, morphology, and thermal analysis of 3d-printed abs-tpu blends by fdm. *J. Vinyl Addit. Technol.* 30 (4), 958–968. doi:10.1002/vnl.22097
- Szust, A., and Adamski, G. (2022). Using thermal annealing and salt remelting to increase tensile properties of 3d fdm prints. *Eng. Fail. Anal.* 132, 105932. doi:10.1016/j. engfailanal.2021.105932
- Tujmer, M., and Pilipović, A. (2025). Effect of annealing on tensile properties of carbon fiber reinforced pa 6 manufactured by fused deposition modeling. *Eur. Mech. Sci.* 9 (1), 8–15. doi:10.26701/ems.1595060
- Vedrtnam, A., Ghabezi, P., Gunwant, D., Jiang, Y., Sam-Daliri, O., Harrison, N., et al. (2023). Mechanical performance of 3d-printed continuous fibre onyx composites for drone applications: an experimental and numerical analysis. *Compos. Part C. Open Access* 12, 100418. doi:10.1016/j.jcomc.2023.100418
- Vorkapić, M., Mladenović, I., Ivanov, T., Kovačević, A., Hasan, M. S., Simonović, A., et al. (2022). Enhancing mechanical properties of 3d printed thermoplastic polymers by annealing in moulds. *Adv. Mech. Eng.* 14 (8), 16878132221120737. doi:10.1177/16878132221120737
- Wang, H., Ding, Z., Chen, X., Liu, H., and Li, N. (2024). Experimental characterisation and constitutive modelling of the intra-ply tensile and shear properties of unidirectional fibre reinforced thermoplastics (ud frtps) under solid-state stamp forming conditions. *Compos. Part A Appl. Sci. Manuf.* 179, 108034. doi:10.1016/j.compositesa.2024.108034
- Wu, Y., Fang, J., Wu, C., Li, C., Sun, G., and Li, Q. (2023). Additively manufactured materials and structures: a state-of-the-art review on their mechanical characteristics and energy absorption. *Int. J. Mech. Sci.* 246, 108102. doi:10.1016/j.ijmecsci.2023.
- Yu, N., Sun, X., Wang, Z., Zhang, D., and Li, J. (2020). Effects of auxiliary heat on warpage and mechanical properties in carbon fiber/abs composite manufactured by fused deposition modeling. *Mater. and Des.* 195, 108978. doi:10.1016/j.matdes. 2020.108978